Electronic Supplementary Material (ESI) for ChemComm.

Supplementary Information

Facile Treatment Tuning the Morphology of Pb with State-of-the-art Selectivity in CO_2 Electroreduction to Formate

Materials and Methods

Materials

CO_2 (purity 99.995%) was supplied by Hangzhou Jingong Special Gas Co. Ltd. (Hangzhou, China). Pb plates (purity 99.99%), used for electrode preparation, were provided by Qinghe County Aoshuo Metal Materials Co., LTD. (Xingtai, Hebei). All other major chemicals such as sodium fluoride (NaF), sodium hydroxide (NaOH), potassium bicarbonate ($KHCO_3$), absolute ethyl alcohol (CH_3CH_2OH) and nitric acid (HNO_3) etc. were of reagent grade and were purchased from Aladdin Reagent Co. Ltd. (Shanghai, China). Acetone was purchased from Huadong Medicine Co. Ltd.

Preparation of the Pb electrodes

The pristine-Pb electrode used in this work was prepared by polishing the commercial lead (Pb) substrate (2 cm * 2 cm) with fine grade emery paper and then ultrasonically cleaned in ethanol and acetone and finally rinsed with deionized water and dried by blowing with N_2 flow.

The treated-Pb electrode was prepared on the basis of polished and cleaned Pb electrode using an electrochemical workstation (CHI760e, CH Instrument, USA) via a successive cyclic voltammetry between -2.0V and 2.0 V cycle 20 weeksat at 0.01 $V•S^{-1}$ rate with 0.001s sampling interval. The cleaned lead plate was used as the working electrode, a saturated calomel electrode was used as the reference electrode and a platinum foil was used as the auxiliary electrode. The electrolyte solution was a mixture of 0.1 $mol·L^{-1}$ HNO_3 and 0.01 $mol·L^{-1}$ NaF in aqueous solution.

Characterization of the electrodes

The surface morphology of the electrode was examined using a field-emission scanning electron microscope (FESEM, S-4800, Hitachi, Japan) under an acceleration voltage of 5 kV. The corresponding crystal phases formed during the roughening process were determined via X-ray diffraction (XRD, XPert Pro MPD, PANalytical, Netherlands) at 45 kV with Cu-Kα radiation.

The surface roughness of the electrodes was obtained by calculating the roughness factor (ρ) according to Eq. (1).

$$\rho = \frac{\int_0^t (I - I\infty)}{\Delta\emptyset \times C \times S} dt \qquad \text{(S1)}$$

where I and I_∞ represent the current and stable current value after a step, respectively, S represents the projected area of the electrodes and C denotes the double-layer capacitance for an ideally smooth electrode, which is equal to 20 μFcm^{-2} ,t = 10 s, and ∅= 5 mV.

Electrochemical reduction of CO_2

Electrochemical reduction of CO_2 was performed in an H-type cell as shown in Scheme S1, the cathodic and anodic chambers were separated by a cation-exchange membrane (Nafion 117, DuPont, USA). Electrolysis of the aqueous solutions containing 0.5 mol L^{-1} NaOH as the anolyte which opens to the air to ensure oxygen formation at low equilibrium potentials, and 0.1 mol L^{-1} $KHCO_3$ with CO_2 saturated as the catholyte, which was stirred continuously with a magnetic stirrer. The electrolyte temperature was controlled at 25℃ using a thermostatic water bath. The as-prepared Pb electrode, a saturated calomel electrode and a platinum foil were used as the working

electrode, reference electrode, and counter electrode, respectively. The working electrode and reference electrode were placed in the cathodic chamber, while the counter electrode was in the anodic chamber. The chronoamperometric response in Figure S2(b) shows that the CO_2RR on treated-Pb is in a steady state after the first 15 min. And therefore gas samples were withdrawn with a gas-tight syringe and analyzed using a gas chromatography (GC, 7890B, Agilent, USA) with HP-MOLESIEVE columns and FID & TCD detectors, and aqueous samples were withdrawn with a syringe and analyzed by an ion chromatography (ICS2000, Dionex, USA) with a Dionex IonPac AS19 Column and a Dionex DS6 detector periodically after the first 15 min. All the potentials were converted to a reversible hydrogen electrode (RHE) scale based on the following equation:

$$E\ (vs.\ RHE) = E\ (vs.\ SCE) + 0.2412\ V + 0.0591\ V \times pH \quad (S2)$$

In addition, iR_u compensation was performed using Eq. (2)

$$E = E\ (vs.\ RHE) - iR_u \quad (S3)$$

where E is the final reported potential, i the average current, and R_u is the uncompensated solution resistance as determined by potentiostatic electrochemical impedance spectroscopy.

The selectivity of the product from CO_2 reduction reaction (CO_2RR) was described using Faradaic efficiency (FE), which was calculated as follows:

$$FE = \frac{z \cdot n \cdot F}{Q} \quad (S4)$$

where z is the electron transfer number, which equals to 2 in the process of formate production, n is the total amount of products in mols, F and Q are the Faraday constant and the quantity of applied electricity.

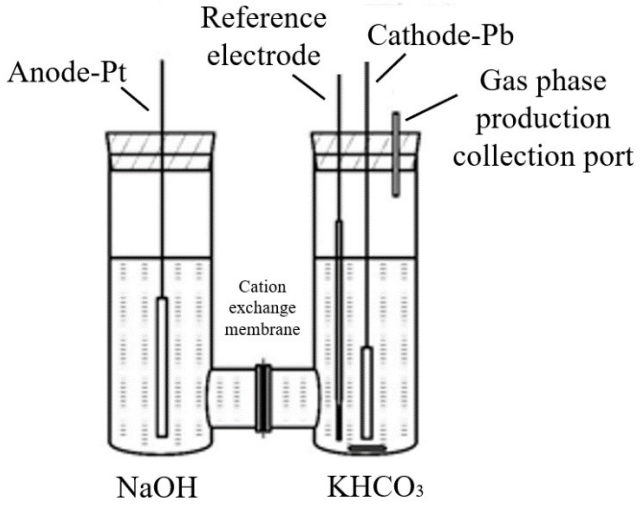

Scheme S1. The sketch map of CO_2 reduction system.

DFT Calculation methods

First principle density functional theory (DFT) calculations in this work were performed by Vienna Ab initio Simulation Package(VASP)[1] with the projector augmented wave (PAW) method[2]. The exchange-functional was treated using the generalized gradient approximation (GGA) of Perdew-Burke-Ernzerhof (PBE)[3] functional. The energy cutoff for the plane wave basis expansion was set to 450 eV and the force on each atom less than 0.03 eV/Å was set as convergence criterion of geometry relaxation. Four-layer with 3×3 and 2×2 supercells were constructed to simulated the Pb (100) and Pb (111) surfaces, respectively, where the bottom two layers were fixed during geometric relaxation. The Brillouin-zone integration was sampled by single Γ point. A convergence energy threshold of 10^{-4} eV was applied in the self-consistent calculations. The free energies of the CO_2 reduction steps were calculated by the

equation[4]: $\Delta G = \Delta E_{DFT} + \Delta E_{ZPE} - T\Delta S$, where ΔE_{DFT} is the DFT electronic energy difference of each step, ΔE_{ZPE} and Δ_S are the correction of zero-point energy and the variation of entropy, respectively, which were obtained by vibration analysis, T is the temperature (T = 300 K).

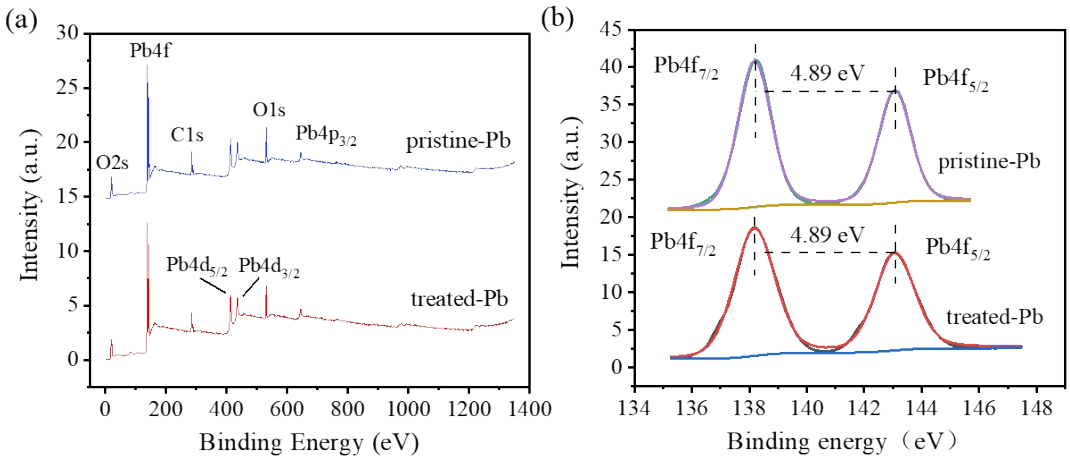

Figure S1. (a) XPS survey and (b) XPS spectra of Pb 4f for pristine-Pb and treated-Pb.

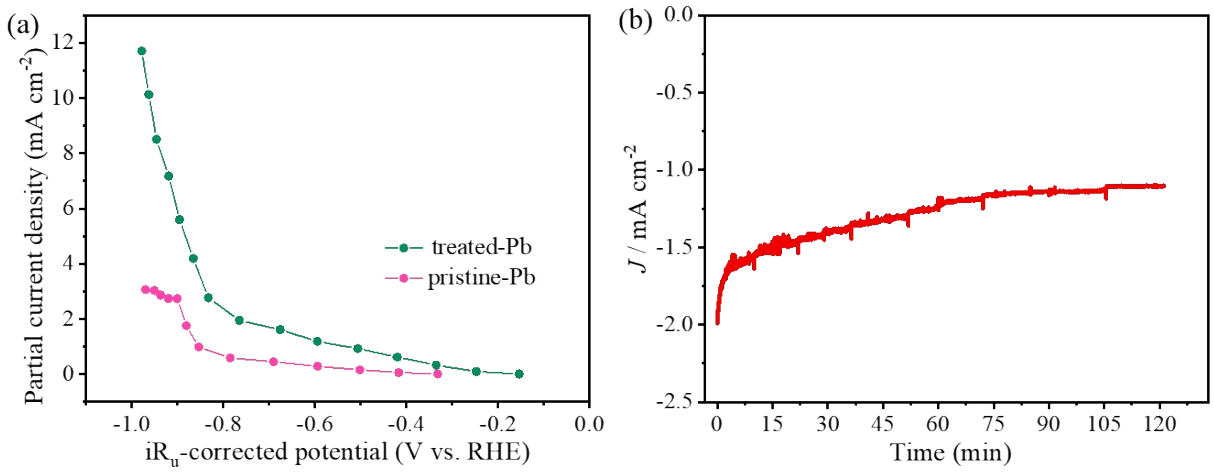

Figure S2. (a) the electrochemical response for formate on the pristine-Pb and treated-Pb electrodes, (b) the chronoamperometric response on treated-Pb at -0.83 V vs. RHE.

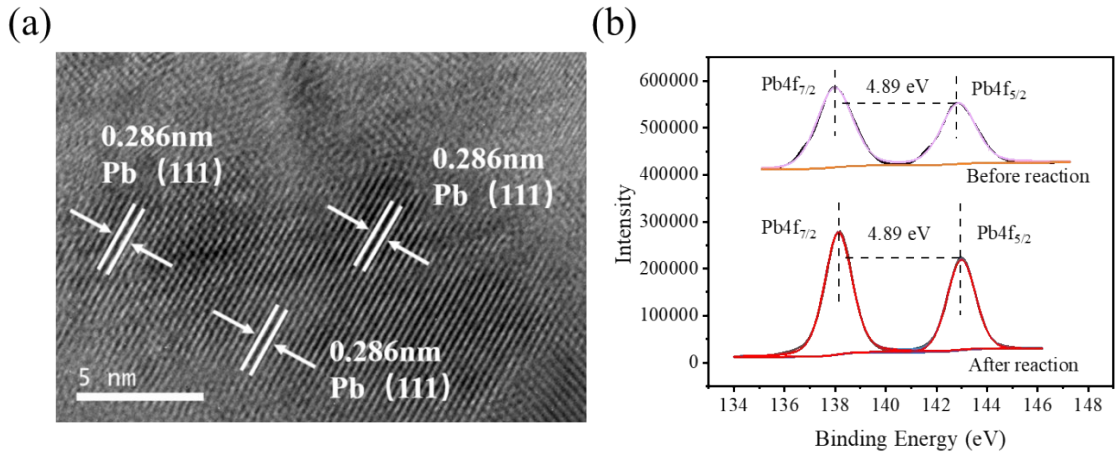

Figure S3. (a) HRTEM image for treated-Pb after five cycles of CO_2RR and (b) XPS spectra of Pb 4f for treated-Pb before and after five cycles of experiments.

Table S1: The comparison in maximum Faradaic efficiency of formate from CO_2RR on different Pb electrodes

Electrocatalysts	Elecrrolytes	Maximum $FE_{formate}$	Potential	Ref.
Pb-plate	0.5 M $NaHCO_3$	55%	−1.61 V versus Ag/AgCl	[5]
Pb granule electrodes	0.2 M K_2CO_3	94%	−1.80 V versus SCE	
sulfide-derived Pb	0.1 M $KHCO_3$	88%	−1.08 V versus SCE	[6]
oxide-derived Pb	0.1 M $KHCO_3$	64%	−1.08 V versus SCE	
Cubic-Pb	0.1 M $KHCO_3$	94.1%	−1.70 V versus Ag/AgCl	[7]
Hexagonal-Pb	0.1 M $KHCO_3$	83.7%	−2.00 V versus Ag/AgCl	
Pristine-Pb	0.1 M $KHCO_3$	55.99%	-0.90 V versus RHE	This work
Treated-Pb	0.1 M $KHCO_3$	**98.03%**	-0.83 V versus RHE	

Table S2: Binding energies (BE) and bond lengths of OCHO* and HCOOH on Pb surfaces

Surfaces	$^{\#1}OCH^{\#2}O$*			$HC^{\#1}O^{\#2}OH$		
	BE(kcal/mol)	$^{\#1}$O-M (Å)	$^{\#2}$O-M(Å)	BE (kcal/mol)	$^{\#1}$O-M (Å)	$^{\#2}$O-M(Å)
Pb(111)	-9.69	2.50	2.48	-2.89	3.43	3.54
Pb(100)	-1.67	2.50	2.49	-0.05	3.53	3.49

Reference

[1] G. Kresse, J. Furthmüller, *Comp. Mater. Sci.* **1996**, *6*, 15-50.

[2] Blöchl, *Physica B.* **1994**, *50*, 17953-17979.

[3] Perdew, Chevary, Vosko, Jackson, Pederson, Singh, Fiolhais, *Physica B* **1992**, *46*, 6671-6687.

[4] S. Egill, B. Thomas, G. Sigrídur, S. Felix, R. Jan, A.-P. Frank, V. Tejs, J. Hannes, N. J. K, *Phys chem. Chem. Phys.* **2012**, *14*, 1235-1245.

[5] F. Köleli, D. Balun, *Appl. Catal A-Gen.* **2004**, *274*, 237-242.

[6] J. E. Pander, J. W. J. Lum, B. S. Yeo, *J. Mater. Chem. A.* **2019**, *7*, 4093-4101.

[7] Y. Kwon, J. Lee, *Electrocatalysis.* **2010**, *1*, 108-115.